Joint EPRI – 123HiMAT International Conference on
Advances in High Temperature Materials
October 21–24, 2019, Nagasaki, Japan
J. Shingledecker, M. Takeyama, editors
https://doi.org/10.31339/asm.cp.am-epri-2019p0570

A UNIQUE INFLUENCE OF CREEP DEFORMATION ON THE SUBSEQUENT FATIGUE CRACK PROPAGATION IN A SINGLE CRYSTAL NI-BASE SUPERALLOY

Shiyu SUZUKI, Motoki SAKAGUCHI, Hirotsugu INOUE
Department of Mechanical Engineering, Tokyo Institute of Technology, Tokyo, JAPAN

ABSTRACT

Single crystal Ni-base superalloys are subjected to tension hold at high temperature in addition to cyclic loading during the operation of gas turbines. Various studies have investigated creep-fatigue crack propagation in superalloys under trapezoidal loadings and evaluated the life time based on parameters such as creep J-integral. However, it is still unclear how damage field and stress-strain condition change at the crack tip during hold time, and how it affects on fatigue crack propagation. In this study, the influence of the tension hold and accompanying creep at crack tip on subsequent fatigue crack propagation behavior was evaluated by introducing single tension holds into pure cyclic loadings. The series of the experiments revealed that because of the tension hold, material degradation and stress relaxation occurred simultaneously ahead of crack tip. In the region where material was degraded, the resistance against crack propagation was reduced, while in the region where stress was relaxed, the crack driving force was lowered.

INTRODUCTION

Single crystal Ni-base superalloy is heat resistant alloy widely used for gas turbine blades for aerospace and power generation industries owing to its excellent balance of creep and fatigue resistance. In these applications, the turbine blades are subjected to fatigue loading due to cyclic thermal stress associated with start-up and shut-down sequence of the gas turbines, and creep loading due to centrifugal loading during steady-state operation. Because of these combined loadings, crack can be initiated and propagates in the material, and then leads to fracture of the components. In order to optimize design and process of inspection and replacement of the turbine blades, it is important to rationalize creep-fatigue crack propagation behavior in Ni-base superalloy.

Creep-fatigue crack propagation in the cast Ni-base superalloys has been investigated for several decades [1-7]. Most of the studies applied trapezoidal loading with holds at max/minimum load of cyclic fatigue loading, and investigate effects of load hold and hold time on the crack propagation behavior. For example, M. Okazaki et al. [1] conducted creep-fatigue crack propagation tests at 950°C using a single crystal Ni-base superalloy, CMSX-2, and revealed that cracks were initiated at microscopic defects such as casting defects in inter-dendritic region, and γ/γ' microstructure was coarsened at crack tip. Furthermore, crack propagation rate based on the number of cycles, da/dN, became higher under creep-fatigue loading than under pure fatigue loading, and longer hold time also increased the da/dN. Similar results have been also reported by V. Lupinc et al. [2, 3], P. Shahinian et al. [4], F. Schubert et al. [5, 6].

Regarding the creep-fatigue crack propagation in typical metallic materials, fracture mechanics parameters which can quantify the crack propagation rate have attracted special interests. Generally, in the case where inelastic region is sufficiently small at crack tip, crack propagation rate can be well evaluated based on linear fracture mechanics parameter, K. This is also the case for creep-fatigue crack propagation in cast Ni-base superalloy, under load hold of several minutes and small scale creep condition [4]. However, if transition from small scale to large scale creep condition occurs with the increase of the hold time, the linear fracture mechanics can no longer be the reasonable measure for crack propagation rate. In this case, creep

J-integral [7] which takes energy dissipation due to the inelastic deformation into account is applicable. The creep J-integral is a parameter modified from the J-integral, replacing the strain field by the strain rate field, and can be experimentally obtained from areas of hysteresis loop of load versus crack tip opening displacement. This parameter is known to be able to evaluate creep fatigue crack propagation rate comprehensively from small scale to large scale creep condition [7].

Although, the previous studies have investigated the creep-fatigue crack propagation in cast Ni-base superalloy under trapezoidal loadings and evaluated crack propagation rates using creep J-integral that expresses macroscopic energy dissipation of specimens, the mechanism of crack propagation which reflects evolution of stress-strain fields and accumulation of damage at the crack tip has not been fully clarified. The aim of this study is to investigate the influence of the creep deformation on the crack propagation in a single Ni-base superalloy, with a special attention to the evolution of stress-strain fields and the accumulation of damage at the crack tip during hold time.

EXPERIMENTAL PROCEDURE

Material and Specimen Preparation

A material used in this study is a single crystal Ni-base superalloy ICMSX-4, which is partially modified from CMSX-4 by excluding element Rhenium. The chemical composition of this material is shown in Table 1. For this material, heat treatments were applied as followed: (1) solution treatment in argon atmosphere at 1277 °C for 2 h, 1288 °C for 2 h, 1296 °C for 3 h, 1304 °C for 3 h, 1313 °C for 2 h, 1316 °C for 2 h, and 1277 °C for 2 h, followed by (2) aging treatment at 1140 °C for 6 h, and 871 °C for 20 h. SEM image of microstructure after the heat treatment is shown in Fig. 1. Average size and volume fraction of cuboidal γ' precipitates were about 0.42 μm and 66%, respectively.

Table 1 Chemical composition of ICMSX-4 (wt%).

Co	Cr	W	Al	Ti	Ta	Mo	Hf	Ni
9.7	6.5	6.4	5.7	1.0	6.6	0.6	0.1	Bal.

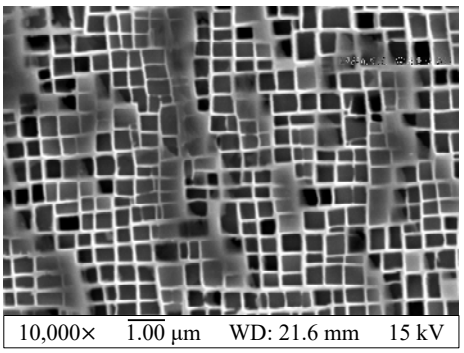

Fig. 1 Microstructure of ICMSX-4.

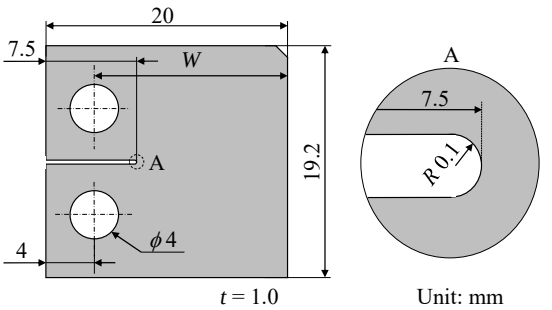

Fig. 2 Geometry of the C(T) specimen.

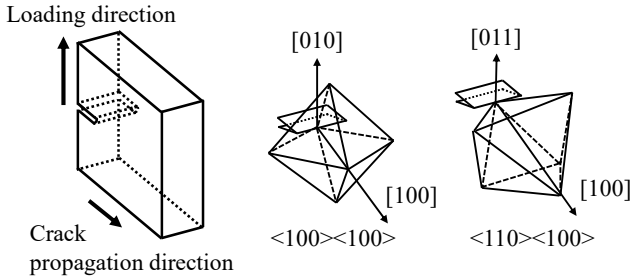

Fig. 3 Schematic illustration of octahedral slip planes in two kinds of specimens.

Compact (C(T)) specimens were manufactured from casting ingots of ICMSX-4 using wire electric discharge machining (EDM) techniques. The ratio of the dimensions of the specimens was designed according to ASTM E647 [8] as shown in Fig. 2. In this study, two types of C(T) specimens of different crystal orientations, <100><100> specimen and <110><100> specimen, were prepared, as shown in Fig. 3. Here, the first and second Miller indices of the specimen names are the primary (in loading direction) and secondary orientation (in crack propagation direction), respectively. For instance, <110><100> specimen has the <110> orientation in the loading direction and <100> orientation in the crack propagation direction.

In this study, most of the tests were conducted using <110><100> specimens. This is because, as reported in our previous study [9, 10], <110><100> specimen shows non-crystallographic crack propagation perpendicular to the loading axis, so that the Mode I symmetric stress distribution can be readily created and reproduced. Contrarily, in <100><100> specimen, crack propagates on crystallographic slip planes being inclined to the loading axis at room temperature, so that it is unlikely for subsequent crack at high temperature to propagate perpendicular to the loading axis.

Creep-fatigue Crack Propagation Test

Creep-fatigue crack propagation tests were conducted at 900°C in air, using an electro-hydraulic machine and an induction heating system. Pre-crack of 0.2 mm length from initial notch tip was introduced into all specimens at room temperatures, under cyclic fatigue loading of constant ΔK condition (ΔK = 15 MPa·m$^{1/2}$). After introducing the pre-crack, specimens were heated up to 900°C, and following loading sequences were applied (Fig. 4);

(i) Cyclic fatigue loading of constant ΔK condition (ΔK = 20 MPa·m$^{1/2}$).
(ii) Tension hold of different K values and hold times.
(iii) Cyclic fatigue loading of ΔK increasing condition restarted from ΔK = 20 MPa·m$^{1/2}$.

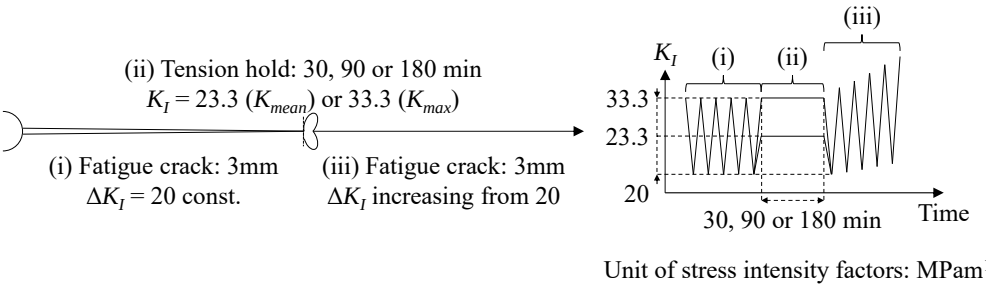

Unit of stress intensity factors: MPam$^{1/2}$

Fig. 4 Schematic illustration of loading conditions.

Table 2 Lists of testing conditions.

Test No.	Crystal orientation	Hold load [MPam$^{1/2}$]	Hold time [min]
(1)	<110><100>	K_{mean} (23.3)	90
(2)		K_{max} (33.3)	90
(3)			30
(4)			180
(5)	<100><100>		90

In the loading sequence (ii), the K value was chosen from K = 23.3 or 33.3 MPa·m$^{1/2}$, which corresponds to mean (K_{mean}) or maximum (K_{max}) value of prior cyclic fatigue loading of ΔK = 20 MPa·m$^{1/2}$ constant, respectively. The tension hold time was chosen from 30, 90 or 180 minutes. Five tests were conducted by changing the crystal orientation, K value and tension hold time, as shown in Table 2. From tests (1) to (4), <110><100> specimens were employed. In test (1), K_{mean} tension hold for 90 minutes was imposed, while in test (2), (3) and (4), K_{max} tension holds for 90, 30 and 180 minutes were imposed, respectively. In test (5), <100><100> specimens were employed, and K_{max} tension hold for 90 minutes was imposed.

For all tests, a load ratio R was 0.4 and a loading frequency was 10 Hz. Cyclic fatigue loading of constant ΔK condition was performed by gradually reducing loading amplitude as crack propagated. The temperature on the specimen's surface was monitored and controlled using type K thermocouple. Temperature distribution in the gauge section of the specimen was arranged within ± 5 °C. Crack length was measured by direct current potential drop (DCPD) method. Furthermore, crack tip on the specimen surface during and after tension hold was observed in-situ using a digital microscope, KEYENCE VHX-5000. Note that creep crack propagation due to the static load during the tension holds was not observed for all tests.

EXPERIMENTAL RESULTS

Effect of *K* Value of Tension Hold

In this section, the effect of the K value of the tension hold on the subsequent fatigue crack propagation was evaluated by comparing the results of test (1) and (2) where <110><100> specimens were employed. Tension holds of K_{mean} =23.3 MPa·m$^{1/2}$ and K_{max} =33.3 MPa·m$^{1/2}$ for 90 minutes were imposed in test (1) and (2), respectively.

Fatigue crack propagation rates, da/dN, obtained in test (1) and (2) were shown in Fig. 5. The horizontal axes indicate projected crack length including initial notch depth. Tension holds were imposed at points indicated by arrows in the figure. Note that fatigue crack propagated from these points after the cyclic fatigue loading was restarted, since creep crack did not propagate during tension holds in this study. As shown in this figure, in test (1) with K_{mean} tension hold, there was no apparent influence of the tension holds on fatigue crack propagation; da/dN gradually increased as ΔK increased from 20 MPa·m$^{1/2}$ soon after the restart of the cyclic fatigue loading. On the other hand, in test (2) with K_{max} tension hold, immediately after the restart of the cyclic fatigue loading, crack propagated for about 40 μm in the similar rate to the prior fatigue loading, then da/dN rapidly decreased to one-hundredth of that under the prior fatigue loading.

Figure 6 shows crack tips observed in-situ by the microscope at the end of the tension hold. Contrary to test (1) (Fig. 6 (a)), strain localization at the crack tip can be observed in the case of test (2) with K_{max} tension hold (Fig 6(b)). The crack tip observed at 200th cycle and 1000th cycle after the restart of the cyclic fatigue loading in this test (2) is shown in Fig. 7. At the 200th cycle, a nascent crack of about 40μm was initiated immediately after the restart of the cyclic fatigue loading, then propagated to 60μm at the 1000th cycle and the da/dN rapidly decreased.

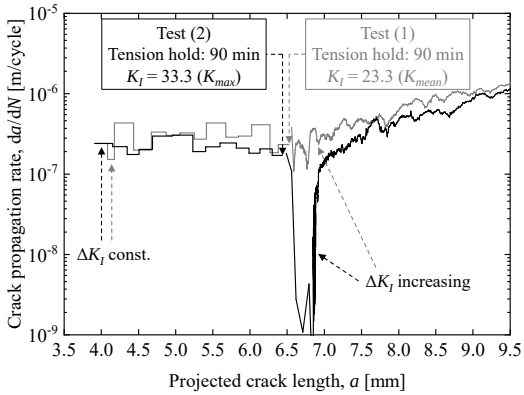

Fig. 5 Comparison of da/dN obtained in test (1) and (2).

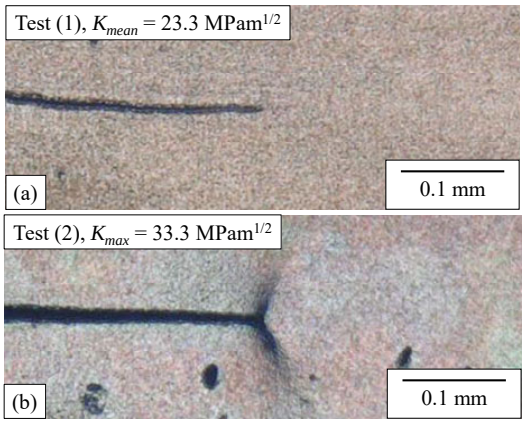

Fig. 6 Crack tips observed in-situ after 90 minutes tension hold in (a) test (1), and (b) test (2).

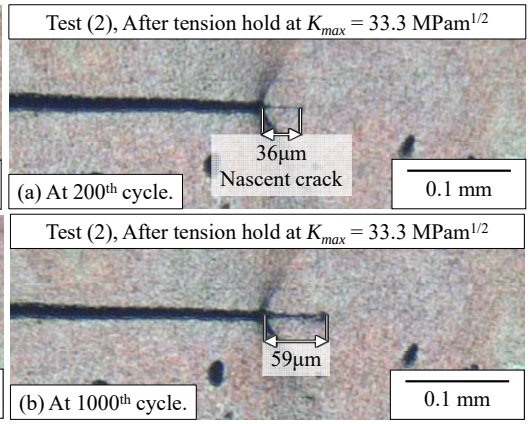

Fig. 7 Crack tips observed in-situ at (a) 200th cycle and (b) 1000th cycle after the restart of the cyclic fatigue loading in the test (2).

Effect of Tension Hold Time

In this section, the effect of the tension hold time on the subsequent fatigue crack propagation was evaluated by comparing the results of test (2), (3) and (4), in which tension holds of K_{max} =33.3 MPa·m$^{1/2}$ for 90, 30 and 180 minutes were imposed, respectively.

Fatigue crack propagation rates, da/dN, obtained in test (2) and (3) were shown in Fig. 8. In test (2) with 90 minutes tension hold, as mentioned above, the da/dN rapidly decreased to one-hundredth of that under the prior fatigue loading. Then the da/dN remained low for a distance of 0.42 mm despite ΔK increased, followed by its rapid acceleration. On the other hand, in test (3) with 30 minutes tension hold, the decrease of the da/dN after the restart of the cyclic fatigue loading was smaller than in test (2). Then the da/dN remained low for a distance of 0.21 mm despite ΔK increased, before its rapid acceleration.

For the next, fatigue crack propagation rates, da/dN, obtained in test (2) and (4) were shown in Fig. 9. In test (4) with 180 minutes tension hold, the decrease of the da/dN after the restart of the cyclic fatigue loading was similar to in test (2), while the distance of the retardation became longer, 0.60 mm.

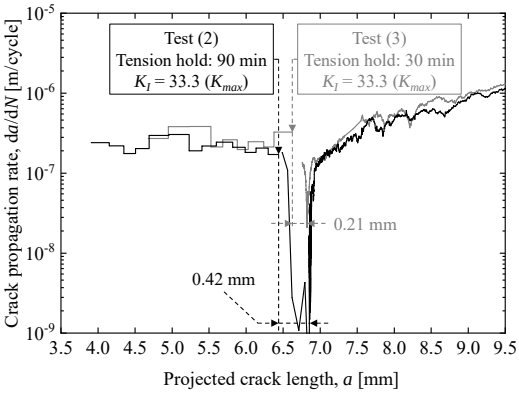

Fig. 8 da/dN obtained in test (2) and (3).

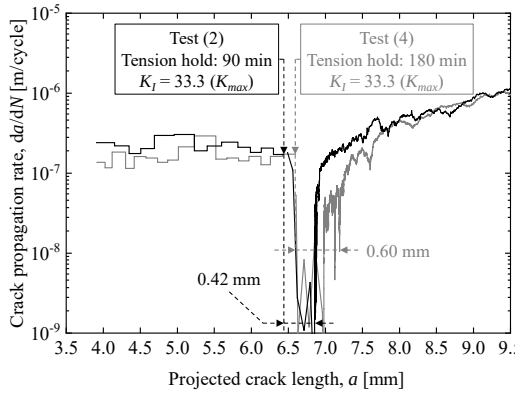

Fig. 9 da/dN obtained in test (2) and (4).

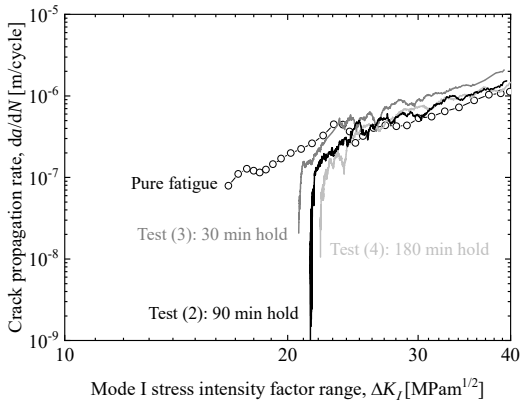

Fig. 10 da/dN under ΔK increasing condition obtained in test (2), (3), (4), and under pure fatigue condition.

The fatigue crack propagation rates under the subsequent fatigue loadings in test (2), (3) and (4) are shown in Fig. 10. Here, data during the significant crack retardation after the restart of the cyclic fatigue loading is excluded, and only that after the rapid acceleration is plotted. Also, da/dN under pure fatigue loading at 900°C in air, which was obtained using the <110><100> specimen, is plotted in the figure as a reference curve. It is clear that in all the tests from (2) to (4), the da/dN after the rapid acceleration converged upon that under the pure fatigue condition.

Effect of Crystal Orientation

Figure 11 shows fatigue crack propagation rates, da/dN, and its crack path obtained in test (5) using <100><100> specimen. Scale of the horizontal axis of the upper graph and the bottom picture were set to be equal. Although the da/dN in this <100><100> specimen under ΔK = 20 MPa·m$^{1/2}$ constant was higher than that of <110><100> specimens, essential phenomenon induced by the tension hold is comparable to that in the case of test (2). Also, it is found that the crack path was inclined to the loading direction, which means the stress distribution at the crack tip should not be dealt with as the typical Mode I crack.

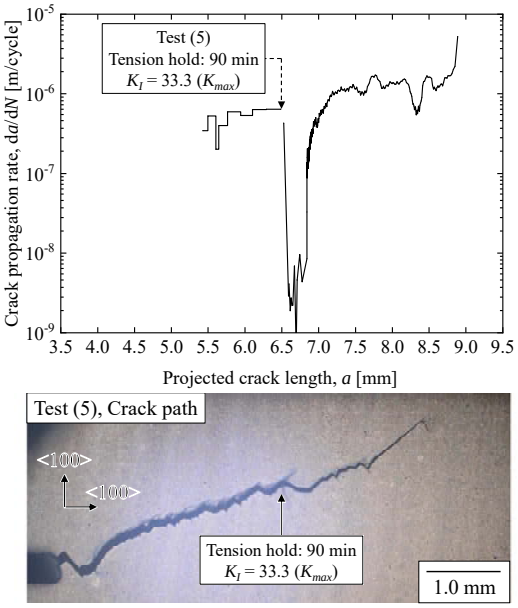

Fig. 11 da/dN and crack path obtained in test (5) using <100><100> specimen.

Table 3 Lists of experimental results.

Test No.	Crystal orientation	Hold load [MPam$^{1/2}$]	Hold time [min]	Strain localization	da/dN after tension hold	Retardation area [mm]
(1)	<110><100>	K_{mean} (23.3)	90	Not observed	No variation	Not observed
(2)		K_{max} (33.3)	90	Observed	1/100	0.42
(3)			30		1/10	0.21
(4)			180		1/100	0.60
(5)	<100><100>		90			0.36

DISCUSSION

The experimental results mentioned in the previous section are listed in Table 3, and summarized as below;

(1) In the case where the tension hold at K_{mean} of the prior cyclic fatigue loading was imposed, no influence of creep was found for the crack propagation rate or crack tip observation.

(2) In the case where the tension hold at K_{max} of the prior cyclic fatigue loading was imposed, the strain localization was observed at the crack tip. After the cyclic fatigue loading was restarted, the da/dN decreased rapidly. Then the da/dN remained low for certain distance despite ΔK increased, followed by its rapid acceleration and convergence on the da/dN under pure fatigue condition.

(3) In the case where the tension hold at K_{max} of the prior cyclic fatigue loading was imposed, the longer hold time resulted in the larger decrease of the da/dN after the restart of the cyclic fatigue loading and the longer distance of the crack retardation.

When crack is subjected to tension hold, tensile creep deformation occurs at crack tip, and (i) material degradation due to void nucleation/growth and (ii) stress relaxation occur simultaneously ahead of crack tip, as shown in Fig. 12. The (i) material degradation reduces crack propagation resistance and increases crack propagation rate, while the (ii) stress relaxation lowers crack driving force and decreases crack propagation rate. Therefore, if creep strain is introduced at crack tip, firstly nascent crack propagation is promoted because of (i). After crack passes through the region where the material is degraded, the effect of (ii) becomes dominant and retards crack propagation. This is the reason for that the nascent crack was immediately initiated after the restart of the cyclic fatigue loading, and the fatigue crack propagation rate rapidly decreased, as described by characteristic (2). Also, after the crack passes through the region where the (ii) stress is relaxed, the da/dN increases and converges on that of healthy material. Moreover, since longer hold time results in larger creep deformation, stress at crack tip is relaxed further and its area becomes broader. Therefore, as described by characteristic (3), the decrease of the da/dN after the restart of the cyclic fatigue loading became larger, and the distance of the retardation became longer. Besides, the crack retardation was not observed in the case of K_{mean} tension hold as described by characteristic (1), possibly because the hold load was not sufficiently large and the creep deformation did not occur at the crack tip as shown in Fig 6.

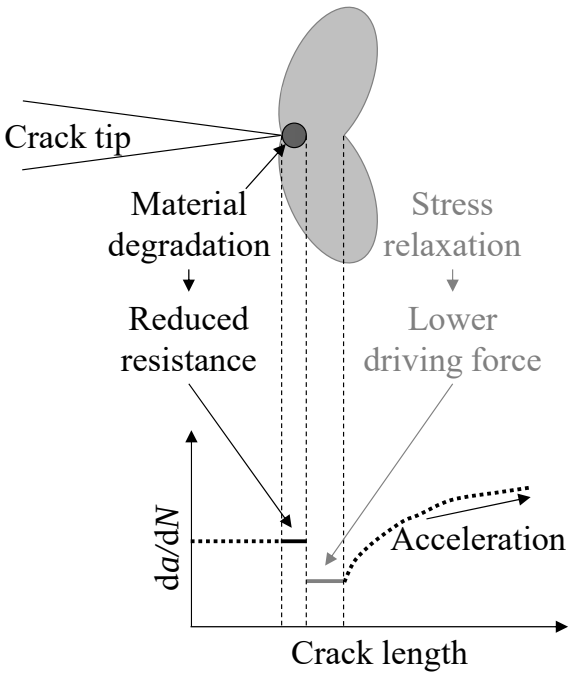

Fig. 12 Schematic illustration of material degradation and stress relaxation at crack tip.

CONCLUSION

In this study, the influence of the creep deformation at the crack tip on the fatigue crack propagation behavior in a single crystal Ni-base superalloy at 900°C was investigated. Creep-fatigue crack propagation tests with the single tension holds imposed during the cyclic fatigue loading were conducted at 900°C, and the effects of hold load and hold time on the subsequent fatigue crack propagation behavior were evaluated. Damage accumulation and evolution of stress-strain fields at crack tip caused by the tension hold, and its influence on the crack propagation were studied. Following conclusions can be drawn;

(1) In the case where the tension hold at K_{mean} of the prior cyclic fatigue loading was imposed, no influence of creep was found on the subsequent crack propagation behavior.

(2) In the case where the tension hold at K_{max} of the prior cyclic fatigue loading was imposed, after the cyclic fatigue loading was restarted, the nascent crack was immediately initiated, then the da/dN decreased rapidly. The da/dN remained low for certain distance, followed by its rapid acceleration and convergence on the da/dN under pure fatigue condition. The longer hold time resulted in the larger decrease of the da/dN after the restart of the cyclic fatigue loading and the longer distance of the crack retardation.

(3) This crack propagation behavior was attributed to the material degradation and the stress relaxation caused by the tension hold. In the region where material was degraded, the resistance against crack propagation was reduced, while in the region where stress was relaxed, the crack driving force was lowered.

The phenomena described in this paper are what observed in single crystal. It is expected that crack propagation behavior depends on stress intensity, hold time and material strength, and results would be very different from this study in poly crystal materials where grain boundary exists.

REFERENCES

[1] M. Okazaki, T. Imai, SI. Nohmi, “Naturally Initiated Fatigue Small Crack Growth in a Single Crystal Ni-Base Superalloy at Elevated Temperature”, Low Cycle Fatigue and Elasto-Plastic Behaviour of Materials—3, Edited by KT. Rie et al., Springer, Dordrecht, (1992), pp. 539-544.

[2] V. Lupinc, G. Onofrio, G. Vimercati, “The Effect of Creep, Oxidation and Crystal Orientation on High Temperature Fatigue Crack Propagation in Standard and Raft-Like Gamma Prime CMSX-2”, Superalloys 1992, Edited by S. D. Antolovich et al., TMS, Warrendale, PA, (1992), pp. 717-726.

[3] V. Lupinc, G. Onofrio, “The effect of creep and oxidation on high-temperature fatigue crack propagation in <001>-loaded CMSX-2 superalloy single crystals”, Materials Science and Engineering A, Vol. 202, No. 1-2, (1995), pp. 76-83.

[4] P. Shahinian, K. Sadananda, “Creep and Fatigue Crack Growth in Several Cast Superalloys”, Superalloys 1984, The Minerals, Metals & Materials Society, (1984), pp. 741-750.

[5] F. Schubert, T. Rieck, P. J. Ennis, “The Growth of Small Cracks in the Single Crystal Superalloy CMSX-4 at 750 and 1000°C”, Superalloys 2000, Edited by T. M. Pollock et al., The Minerals, Metals & Materials Society, Warrendale, PA, (2000), pp. 341-346.

[6] F. Schubert, H. J. Penkalla, P. J. Ennis, L. Singheiser, “Crack Growth Behaviour of Nickel-Base High Temperature Alloys at 500 to 1000°C”, International Conference on Fracture, (2001).

[7] S. Taira, R. Ohtani, T. Komatsu, “Application of J-Integral to High-Temperature Crack Propagation: Part II—Fatigue Crack Propagation”, Journal of Engineering Materials and Technology, Vol. 101, (1979), pp. 162-167

[8] “Standard Test Method for Measurement of Fatigue Crack Growth Rates”, Annual Book of ASTM Standards E647-08, ASTM International, (2010), pp. 669-713.

[9] S. Suzuki, M. Sakaguchi, H. Inoue, “Temperature dependent fatigue crack propagation in a single crystal Ni-base superalloy affected by primary and secondary orientations”, Materials Science and Engineering: A, Vol. 724, (2018), pp. 559-565.
[10] M. Sakaguchi, R. Komamura, X. Chen, M. Higaki, H. Inoue, “Crystal plasticity assessment of crystallographic Stage I crack propagation in a Ni-based single crystal superalloy”, International Journal of Fatigue, Vol. 123, (2019), pp.10-21.